$$\text{Goodness of Fit (\%)} = 100 \times \left[1 - \left(\sum_{m=1}^{N} \frac{|H_{model}(f) - H_{est}(f)|^2}{m}\right) \Big/ \left(\sum_{m=1}^{N} \frac{|H_{est}(f)|^2}{m}\right)\right]$$

$$f = f_0 \times m$$

where f_0, m, and N represent the fundamental frequency of the Fourier transformation, a frequency index, and the number of data points used for the fitting, respectively. When $H_{model}(f)$ is zero for all of the frequencies, the goodness of fit is zero. When $H_{model}(f)$ equals $H_{est}(f)$ for all of the frequencies, the goodness of fit is 100%.

To facilitate intuitive understanding of the dynamic characteristics described by the transfer function (see Appendix A for details), we calculated the step response from the corresponding transfer function as follows. An impulse response of the system was calculated using the inverse Fourier transformation of the estimated transfer function. The step response was then obtained from the time integral of the impulse response. The steady-state response was calculated by averaging the last 10 s of data from the step response. The 80% rise time for the sympathetic step response or the 80% fall time for the vagal step response was estimated as the time at which the step response reached 80% of the steady-state response.

Statistics. All data are presented as means and SD values. Mean values of HR, AP, and CSNA as well as parameters of the transfer functions and step responses were compared between the control and ANG II conditions using paired *t*-tests. Differences were considered significant when $P < 0.05$ (11).

RESULTS

Typical recordings of the vagal stimulation command, HR, and AP obtained under control and ANG II conditions are shown in Fig. 1*A*. The random vagal stimulation began at 60 s. The HR decreased in response to the random vagal stimulation. ANG II, which did not affect the prestimulation baseline HR, attenuated the magnitude of the vagal stimulation-induced variations in HR. ANG II increased the AP both before and during the vagal stimulation. ANG II did not change the prestimulation or poststimulation CSNA (Fig. 1*B*).

As shown in Table 1, ANG II did not affect the mean HR before stimulation of the vagal nerve, whereas it significantly increased the mean HR during the vagal stimulation period. ANG II attenuated the reduction in HR, which was calculated as the difference between the prestimulation HR and the mean HR observed during the vagal stimulation period. ANG II significantly increased the mean AP both before and during the vagal stimulation period. ANG II did not affect the mean level of pre- or poststimulation CSNA significantly.

Figure 2*A* illustrates the averaged transfer functions from vagal stimulation to HR obtained under the control and ANG II conditions. In the gain plots, the transfer gain was relatively constant for frequencies below 0.1 Hz and decreased as the frequency increased above 0.1 Hz. ANG II decreased the transfer gain for all of the investigated frequencies, resulting in

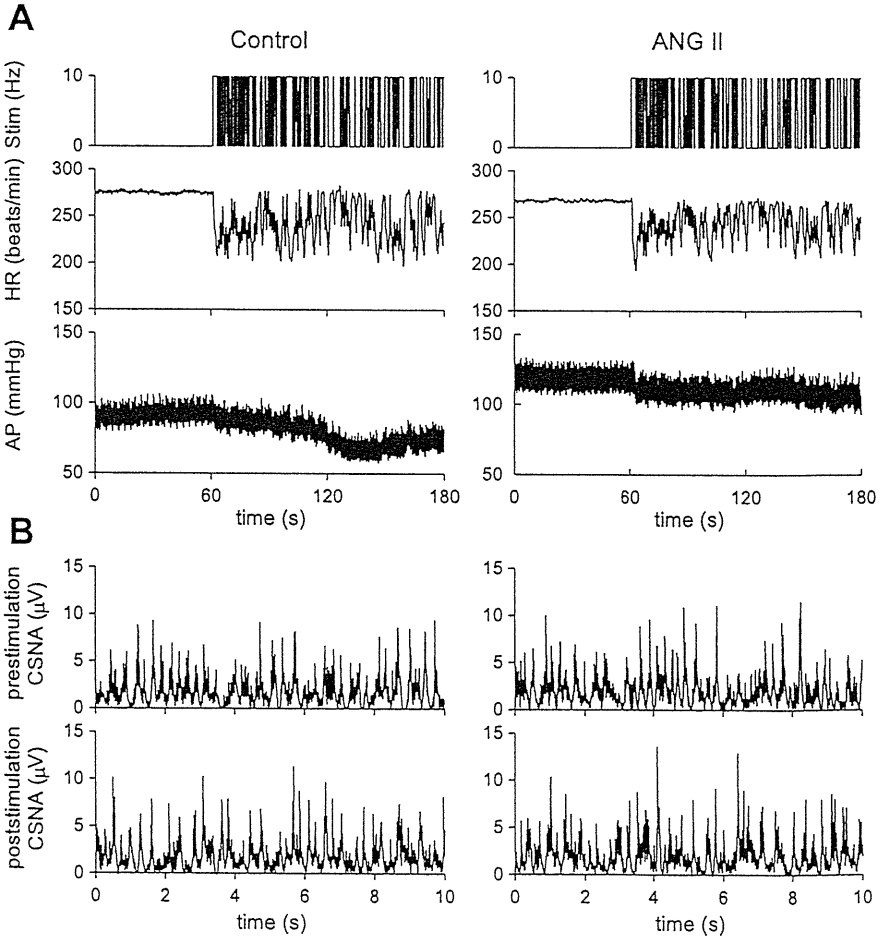

Fig. 1. *A*: representative recordings of vagal nerve stimulation (Stim), the heart rate (HR), and arterial pressure (AP). The *left* and *right* panels show recordings obtained before and during intravenous administration of angiotensin II (ANG II; 10 $\mu g \cdot kg^{-1} \cdot h^{-1}$), respectively. The amplitude of the HR variation in response to vagal stimulation was smaller in the presence of ANG II compared with results obtained without ANG II. *B*: representative recordings of cardiac sympathetic nerve activity (CSNA) under prestimulation baseline and poststimulation conditions. ANG II did not affect the CSNA significantly.

Table 1. *Mean values for HR, AP, and CSNA obtained using the vagal stimulation protocol*

	Control	ANG II	*P* Value
HR, beats/min			
Prestimulation	278±21	281±31	0.60
During stimulation	232±19	245±26*	0.046
Difference‡	−46±6	−37±10†	0.0017
AP, mmHg			
Prestimulation	91±23	127±17†	0.0057
During stimulation	85±24	118±19†	0.0055
Difference‡	−6.3±9.2	−9.2±8.6	0.34
CSNA, μV			
Prestimulation	1.21±0.38 (100%)	1.19±0.46 (98±15%)	0.82
Poststimulation	1.27±0.42 (105±8%)	1.20±0.55 (98±27%)	0.59

Data are means ± SD values; $n = 7$. HR, heart rate; AP, arterial pressure; CSNA, cardiac sympathetic nerve activity. ‡The difference was calculated by subtracting the prestimulation value from the value obtained during the vagal stimulation period in each animal. *$P < 0.05$ and †$P < 0.01$ based on a paired *t*-test. Exact *P* values are also shown.

a parallel downward shift in the gain plot. In the phase plots, the phase approached $-\pi$ radians at 0.01 Hz and the lag became larger as the frequency increased. ANG II did not alter the phase characteristics significantly. In the coherence plots, the coherence value was close to unity in the frequency range from 0.01 to 0.8 Hz. The sharp variation around 0.6 Hz corresponds to the frequency of the artificial ventilation. Figure 2*B* depicts the HR step responses calculated from the corresponding transfer functions. ANG II significantly attenuated the steady-state response without affecting the response speed.

As shown in Table 2, ANG II significantly attenuated the dynamic gain of the vagal transfer function to 76.1 ± 8.5% of the control value without affecting the corner frequency or pure delay. The goodness of fit to the first-order low-pass filter did not differ between the control and ANG II conditions. In the HR step response, ANG II significantly attenuated the steady-state response without affecting the 80% fall time.

Typical recordings of the sympathetic stimulation command, HR, and AP obtained under control and ANG II conditions are shown in Fig. 3*A*. The random sympathetic stimulation began at 60 s. HR increased in response to random sympathetic stimulation. ANG II did not affect the prestimulation baseline HR. The magnitude of the HR variation in response to sympathetic stimulation did not change significantly. ANG II increased the AP both before and during the sympathetic stimulation. ANG II did not change the pre- or poststimulation CSNA significantly (Fig. 3*B*).

As shown in Table 3, ANG II did not affect the mean HR before or during the period of sympathetic stimulation. ANG II did not affect the increase in HR, calculated as the difference between the prestimulation HR and the mean HR in response to sympathetic stimulation. ANG II significantly increased the mean AP both before and during the sympathetic stimulation period. ANG II did not affect the mean level of pre- or poststimulation CSNA significantly.

Figure 4*A* illustrates the averaged transfer functions from sympathetic stimulation to HR obtained under control and ANG II conditions. In the gain plots, the transfer gain decreased as the frequency increased. ANG II did not change the transfer gain markedly. In the phase plots, the phase ap-

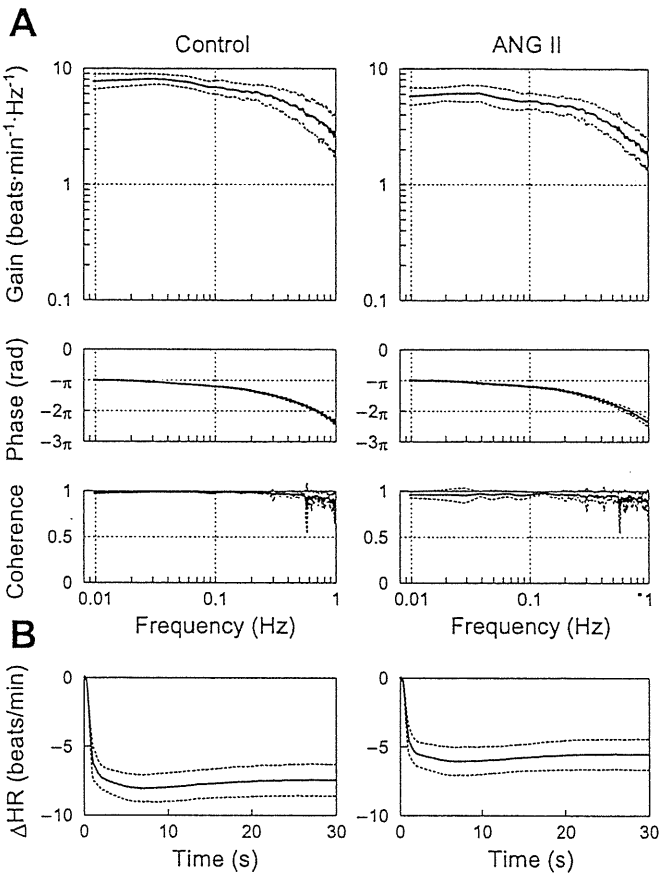

Fig. 2. *A*: averaged transfer functions from vagal nerve stimulation to the HR response obtained before and during intravenous administration of ANG II. Gain plots (*top*), phase plots (*middle*), and coherence plots (*bottom*) are shown. ANG II caused a parallel downward shift in the gain plot. ANG II did not affect the phase plot or coherence plot significantly. *B*: step responses of the HR to a unit change in the vagal stimulation calculated from the corresponding transfer functions. ANG II significantly attenuated the step response of the HR. ΔHR, changes in heart rate. Solid lines indicate mean, and dashed lines indicate mean ± SD.

proached zero radians at 0.01 Hz and increasingly lagged as the frequency increased. ANG II did not affect the phase characteristics significantly. The coherence value was above 0.9 for the frequency range below 0.1 Hz and decreased in the frequency range above 0.1 Hz. Figure 4*B* depicts the HR step responses calculated from the corresponding transfer functions. ANG II did not affect the steady-state response or the response speed.

Table 2. *Effects of ANG II on the parameters of the transfer function and the step response relating to the dynamic vagal control of HR*

	Control	ANG II	*P* Value
Dynamic gain, beats·min^{-1}·Hz^{-1}	7.6±0.9	5.8±0.9*	0.00042
Corner frequency, Hz	0.39±0.12	0.36±0.10	0.12
Pure delay, s	0.48±0.04	0.47±0.06	0.82
Goodness of fit, %	98.8±0.4	98.6±0.8	0.63
Steady-state response, beats/min	−7.4±1.1	−5.6±1.1*	0.0011
80% Fall time	1.31±0.31	1.33±0.37	0.60

Data are means ± SD values; $n = 7$. *$P < 0.01$ based on a paired *t*-test. Exact *P* values are also shown.

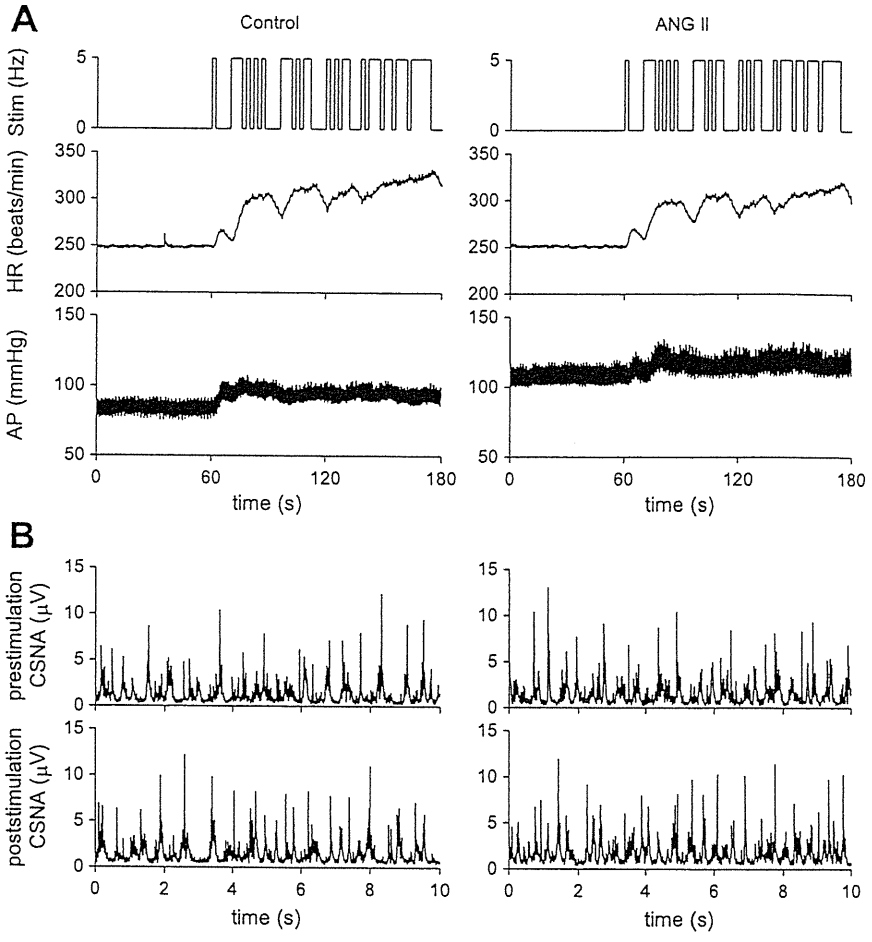

Fig. 3. *A*: representative recordings of cardiac sympathetic nerve stimulation (Stim), HR, and AP. The *left* and *right* panels show the recordings before and during intravenous administration of ANG II (10 $\mu g \cdot kg^{-1} \cdot h^{-1}$), respectively. The amplitude of the HR variation during sympathetic stimulation was unchanged by the addition of ANG II. *B*: representative recordings of CSNA under prestimulation baseline and poststimulation conditions. ANG II did not affect the CSNA significantly.

As shown in Table 4, ANG II slightly attenuated the dynamic gain of the sympathetic transfer function to 92.5 ± 8.9% of the value observed under control conditions. ANG II did not affect the natural frequency, damping ratio, or pure delay. The goodness of fit to the second-order low-pass filter did not differ between the control and ANG II conditions. In the HR step response, ANG II did not affect the steady-state response or the 80% rise time. As shown in Table 5, there were no significant differences in the parameters of the sympathetic transfer function between repeated estimations with an intervening interval of more than 20 min.

Table 3. *Mean values for HR, AP, and CSNA obtained using the sympathetic stimulation protocol*

	Control	ANG II	*P* Value
HR, beats/min			
Prestimulation	267±16	261±19	0.21
During stimulation	317±26	311±23	0.063
Difference†	50±21	50±21	0.94
AP, mmHg			
Prestimulation	74±6	106±15*	0.0011
During stimulation	78±6	110±17*	0.0023
Difference†	4.7±3.6	4.1±5.4	0.71
CSNA, μV			
Prestimulation	0.91±0.71 (100%)	0.98±0.78 (99±19%)	0.22
Poststimulation	0.93±0.72 (101±4%)	1.02±0.81 (104±21%)	0.18

Data are means ± SD values; $n = 7$ except for CSNA data where $n = 5$. †The difference was calculated by subtracting the prestimulation value from the value obtained during the sympathetic stimulation period in each animal. *$P < 0.01$ based on a paired *t*-test. Exact *P* values are also shown.

DISCUSSION

Intravenous administration of ANG II at 10 $\mu g \cdot kg^{-1} \cdot h^{-1}$ increased AP but did not affect mean HR or mean CSNA during prestimulation baseline conditions (Tables 1 and 3), suggesting that ANG II at this dose did not affect the residual sympathetic tone to the heart significantly. ANG II significantly attenuated the dynamic gain of the transfer function from vagal stimulation to HR, whereas it only slightly attenuated that of the transfer function from sympathetic stimulation to HR (Tables 2 and 4).

Effects of ANG II on the transfer function from vagal stimulation to HR. ANG II attenuated the dynamic gain of the transfer function from vagal stimulation to HR without affecting the corner frequency or pure delay (Fig. 2 and Table 2). Several interventions can affect the dynamic gain of the vagal transfer function and significantly change the corner frequency. For example, inhibition of cholinesterase, which interferes with the rapid hydrolysis of ACh, augments the dynamic gain and decreases the corner frequency (29). Moreover, blockade of muscarinic K^+ channels, which interferes with fast, membrane-delimited signal transduction, has been shown to attenuate the dynamic gain and decrease the corner frequency (26).

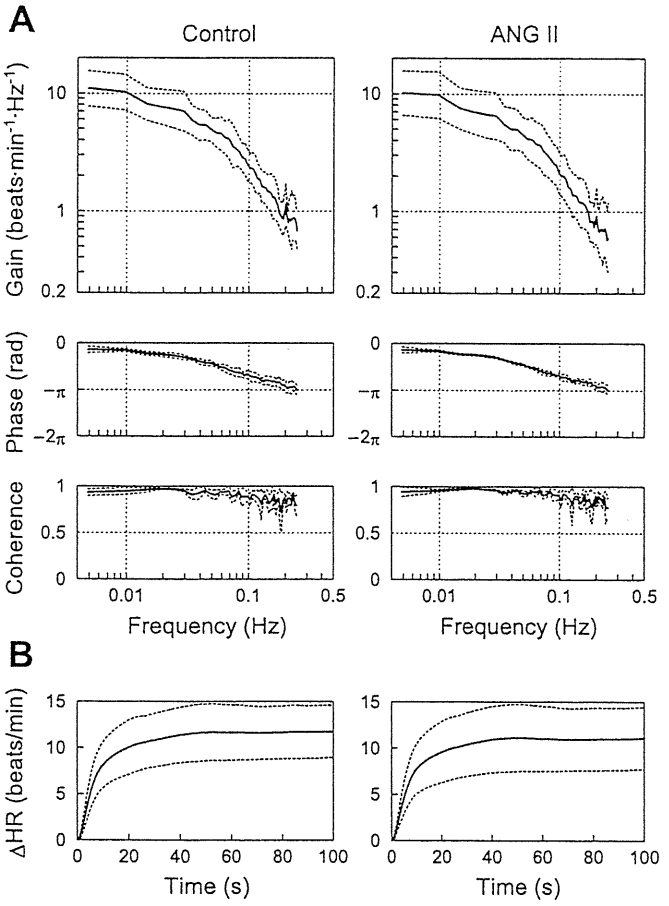

Fig. 4. *A*: averaged transfer functions from cardiac sympathetic nerve stimulation to the HR response obtained before and during intravenous administration of ANG II. Gain plots (*top*), phase plots (*middle*), and coherence plots (*bottom*) are shown. *B*: step responses of the HR to a unit change in the sympathetic stimulation calculated using the transfer functions. ΔHR, changes in heart rate. Solid lines indicate mean, and dashed lines indicate mean ± SD.

On the other hand, several other interventions have been shown to alter the dynamic gain of the vagal transfer function without changing the corner frequency. Concomitant cardiac sympathetic nerve stimulation or increased intracellular cyclic AMP levels augments the dynamic gain without affecting the corner frequency (14, 27), whereas β-adrenergic blockade or high plasma NE attenuates the dynamic gain without affecting the corner frequency (24, 25). Because α-adrenergic blockade nullifies its effects, high plasma NE probably functions via

Table 4. *Effects of intravenous ANG II administration on the parameters of the transfer function and the step response relating to the dynamic sympathetic control of HR*

	Control	ANG II	*P* Value
Dynamic gain, beats·min^{-1}·Hz^{-1}	10.8±2.6	10.2±3.1*	0.049
Natural frequency, Hz	0.069±0.009	0.065±0.006	0.090
Damping ratio	1.53±0.25	1.48±0.21	0.26
Pure delay, s	0.51±0.31	0.42±0.18	0.20
Goodness of fit, %	97.0±1.6	96.9±1.7	0.67
Steady-state response, beats/min	11.8±2.8	11.1±3.4	0.052
80% Rise time, s	17.2±4.7	16.8±4.5	0.62

Data are means ± SD; $n = 7$. *$P < 0.05$ based on a paired *t*-test. Exact *P* values are also shown.

Table 5. *Time effects on the parameters of the transfer function and the step response relating to the dynamic sympathetic control of HR*

	Control 1	Control 2	*P* Value
Dynamic gain, beats·min^{-1}·Hz^{-1}	9.1±1.7	8.6±2.4	0.37
Natural frequency, Hz	0.062±0.014	0.065±0.017	0.10
Damping ratio	1.36±0.22	1.34±0.28	0.75
Pure delay, s	0.65±0.32	0.56±0.25	0.12
Goodness of fit, %	95.8±4.0	97.3±2.2	0.32
Steady-state response, beats/min	9.8±2.0	9.5±2.8	0.55
80% Rise time, s	15.7±3.4	14.4±3.8	0.37

Data are means ± SD; $n = 7$. Exact *P* values are shown.

α-adrenergic receptors on preganglionic and/or postganglionic vagal nerve terminals to limit ACh release during vagal stimulation (24). Our observation that ANG II attenuated the dynamic gain without affecting the corner frequency or pure delay is similar to the results observed with high plasma NE, suggesting that ANG II limits ACh release during vagal stimulation. Although estimated values of the corner frequency ranged from 0.1 to 0.4 among studies, the difference may be attributable to the difference in the input signal properties (see Appendix B for details).

Although Andrews et al. (2) reported that ANG II (500 ng/kg, iv bolus) did not inhibit vagally induced bradycardia in anesthetized ferrets, Potter (31) demonstrated that ANG II (5–10 μg, iv bolus; body weight not shown) attenuated vagally induced bradycardia in anesthetized dogs. The latter study also showed that the addition of ANG II (2–5 μg/25 ml) to an organ bath attenuated vagally induced bradycardia in isolated guinea-pig atria. In that study, ANG II did not attenuate ACh-induced bradycardia, suggesting that the inhibition of bradycardia by ANG II was due to an inhibition of ACh release from vagal nerve terminals (31). In a previous study, we confirmed that intravenous ANG II (10 μg·kg^{-1}·h^{-1}) attenuated myocardial interstitial ACh release in response to vagal nerve stimulation in anesthetized cats (17). The site of this inhibitory action was thought to be parasympathetic ganglia rather than postganglionic vagal nerve terminals, because losartan, an antagonist of the ANG II receptor subtype 1 (AT_1 receptor), abolished the inhibitory action of ANG II when it was administered intravenously but not when it was administered locally through a dialysis fiber. ANG II may also function at the coronary endothelium and produce a diverse range of paracrine effects (6). Although the exact mechanisms remain to be elucidated, intravenous ANG II inhibits ACh release and thereby attenuates the dynamic gain of the vagal transfer function without affecting the corner frequency or pure delay.

Although the observed attenuation of the dynamic HR response to vagal stimulation by ANG II is relatively small, it may have pathophysiological significance as follows. In a previous study, our laboratory has shown that chronic intermittent vagal stimulation significantly improved the survival of chronic heart failure rats after myocardial infarction (21). In that study, the vagal stimulation intensity was such that it reduced HR only by 20 to 30 beats/min (5–10%) in rats. Therefore, change in the vagal effects on the heart, even if relatively small, could affect the evolution of heart failure. Increased plasma or tissue levels of ANG II in heart failure

might attenuate vagal neurotransmission, contributing to the aggravation of disease states.

Effects of ANG II on the transfer function from sympathetic stimulation to HR. Although ANG II attenuated the dynamic gain of the transfer function from sympathetic stimulation to HR without affecting the natural frequency, damping ratio, or pure delay, the attenuating effect was not definitive because the effect was not significant on the steady-state response in the calculated step response (Fig. 4 and Table 4). There are conflicting reports about the effects of ANG II on sympathetic control of the heart. Starke (33) reported that ANG II (1 ng/ml) potentiated NE release in response to postganglionic sympathetic nerve stimulation in isolated rabbit hearts, whereas no effect on spontaneous or tyramine-induced NE output was observed. Farrell et al. (10) demonstrated that administration of ANG II (100 μM at 1 ml/min for 10 min; ~35–42 $\mu g \cdot kg^{-1}$) into right atrial ganglionated plexus neurons via a branch of the right coronary artery caused the release of catecholamine into the myocardial interstitial fluid of anesthetized dogs, suggesting that ANG II affects intrinsic cardiac neurons. In that study, the effect of ANG II on the catecholamine release induced by cardiac sympathetic nerve stimulation was not investigated. On the other hand, Lameris et al. (19) demonstrated that administration of ANG II (0.5 $ng \cdot kg^{-1} \cdot min^{-1}$ or 30 $ng \cdot kg^{-1} \cdot h^{-1}$) into the left anterior descending coronary artery of anesthetized pigs did not yield spontaneous NE release or enhance the NE release induced by cardiac sympathetic nerve stimulation. Cardiac ganglia derived from different species can demonstrate differences in phenotype for ANG II receptors, and this may impact on the resultant neurohumoral interactions. Dendorfer et al. (7) demonstrated that ANG II (0.3 to 1 μg/kg bolus) increased renal sympathetic nerve activity during ganglionic blockade in pithed rats, suggesting direct ganglionic excitation by ANG II. In the present study, because we stimulated the postganglionic cardiac sympathetic nerve, possible direct ganglionic excitation by ANG II might not have affected the dynamic sympathetic control of HR. In addition, postganglionic CSNA did not change significantly in our experimental conditions (Tables 1 and 3), indicating that the 10 $\mu g \cdot kg^{-1} \cdot h^{-1}$ dose of intravenous ANG II was not high enough to produce direct ganglionic excitation.

In isolated rabbit hearts, Peach et al. (30) demonstrated that ANG II (0.2 ng/ml) inhibited NE uptake. Starke (33) reported a higher dose of ANG II (10 μg/ml) to inhibit NE uptake. In a previous study from our laboratory, blockade of neuronal NE uptake using desipramine attenuated the dynamic gain, decreased the natural frequency, and increased the pure delay of the transfer function from sympathetic stimulation to HR (28). In the present study, however, neither the natural frequency nor the pure delay was changed by ANG II, suggesting that NE uptake was not inhibited. In an in vivo study using canine hearts, Lokhandwala et al. (22) demonstrated that ANG II (100 and 200 $ng \cdot kg^{-1} \cdot min^{-1}$ or 6 and 12 $\mu g \cdot kg^{-1} \cdot min^{-1}$ iv) did not affect the positive chronotropic effects of either postganglionic cardiac sympathetic nerve stimulation or intravenous NE infusion. In that study, ANG II enhanced the positive chronotropic effects of sympathetic nerve stimulation but not of intravenous NE infusion after blocking neuronal NE uptake with desipramine. The authors' interpretation of the results was that ANG II facilitated NE release in response to sympathetic nerve stimulation, whereas any effects of ANG II might be masked in animals with functioning neuronal NE uptake mechanisms (22). To make matters more complex, Lameris et al. (19) did not observe enhanced NE release during cardiac sympathetic stimulation in porcine hearts even after neuronal NE uptake was blocked with desipramine. Thus it appears that differences in species, ANG II doses, and experimental settings (in vivo vs. isolated hearts, intravenous vs. intracoronary administration, with or without the contribution of sympathetic ganglia) critically affected the experimental results. Therefore, we believe that assessing the relative effects of ANG II on the vagal and sympathetic systems is important to understand the pathophysiological roles of ANG II in the autonomic regulation of HR.

Limitations. Our results should be interpreted in the context of various experimental limitations. First, we obtained data from anesthetized animals. If the data had been obtained under conscious conditions, the results might have been different. Because we disabled the arterial baroreflexes and cut the autonomic efferent pathways, however, the anesthetics should not have markedly affected our results. Second, because we stimulated the postganglionic cardiac sympathetic nerve, the possible effects of ANG II on the sympathetic ganglia were not assessed. Further studies that stimulate the preganglionic cardiac sympathetic nerve with various doses of ANG II are required to determine the effects of ANG II on the cardiac sympathetic ganglionic transmission. Finally, ANG II may affect the autonomic regulation of HR chronically. Further studies focused on the effects of chronically elevated ANG II levels on the autonomic regulation of HR are required to elucidate the pathophysiological significance of elevated ANG II levels.

In conclusion, continuous intravenous administration of ANG II at a dose that did not induce direct cardiac sympathetic ganglionic excitation significantly attenuated the dynamic gain of the transfer function from vagal stimulation to HR. The attenuation of the transfer gain was observed uniformly in the frequency range under study, suggesting that ANG II can attenuate the HF component of HRV even when vagal outflow from the central nervous system remains unchanged. In addition, the same dose of ANG II did not markedly affect the dynamic gain of the transfer function from postganglionic sympathetic stimulation to HR. Although there remains a room for arguments relating to the different site of stimulation (preganglionic for vagal vs. postganglionic for sympathetic), possible disproportional suppression of the dynamic vagal and sympathetic regulation of HR likely results in a relative dominance of sympathetic control in the presence of ANG II. Because many neurohumoral elements remodel or adapt during the evolution of cardiac pathology (18), we cannot directly extrapolate the results of acute neurohumoral interactions observed in the present study to the chronic pathological situations. If we do so, however, the reduction of the HF component of HRV in patients with cardiovascular diseases, such as myocardial infarction and heart failure (34), may be partly explained by the peripheral effects of ANG II on the dynamic autonomic regulation of HR.

APPENDIX A

Meaning of a step response calculated from a transfer function. We calculated a step response from a transfer function relating to the vagal or sympathetic HR control. The calculated step response is useful for time-domain interpretation of the low-pass filter characteristics described by the frequency-domain transfer function but does not necessarily conform to an experimentally estimated step response because of the following reasons. The transfer function identifies the

linear input-output relationship of a given system around a mean input signal (5 Hz for vagal and 2.5 Hz for sympathetic stimulation in the present study). The step response is then calculated for a unit change in the input signal. If we perform a kind of experiment where we change the stimulation frequency from 4.5 to 5.5 Hz for the vagal system and from 2 to 3 Hz for the sympathetic system, the resultant step response is most likely close to the calculated step response. The ordinary experimental step response is, however, estimated by a step input in which the stimulation is completely turned off before the stimulation starts. The calculated step response and the ordinary experimental step response can conform only when the system is purely linear. Whenever nonlinearities exist such as threshold and saturation commonly observed in biological systems, the two step responses disagree. Conversely, information gained by the ordinary experimental step response has a limited ability to estimate the dynamic HR response unless the system is purely linear.

Once vagal or sympathetic transfer function is identified, an impulse response of the system is obtained by an inverse Fourier transform of the transfer function. We can estimate the dynamic HR response from a convolution of a input signal and the impulse response. Figure 5 represents typical data of measured HR and calculated HR based on the transfer function. Figure 5*A* is a continuation of the time series obtained under the control condition depicted in Fig. 1*A*. Figure 5*B* shows a scatter plot of measured HR versus calculated HR during dynamic vagal stimulation. The solid line indicates a linear regression line ($r^2 = 0.94$). Figure 5*C* is a continuation of the time series obtained under the control condition depicted in Fig. 3*A*. Figure 5*D* shows the scatter plot of measured HR versus calculated HR during dynamic sympathetic stimulation. The solid line indicates a linear regression line. Although a slight convex nonlinearity is noted between the measured HR and calculated HR, squared correlation coefficient is high ($r^2 = 0.89$). These results indicate that the transfer function can represent the dynamic HR response reasonably well.

APPENDIX B

Binary white noise versus Gaussian white noise. In a previous study from our laboratory (29), we reported a corner frequency of ~0.1 Hz for a transfer function from vagal stimulation to HR, which was distinctly different from the result of the present study. Possible explanation for the discrepancy is the difference in the input variance (or power) of vagal stimulation. In the previous study, we used a Gaussian white noise (GWN) with a mean stimulation frequency of 5 Hz and a SD of 2 Hz so that the input signal covered at most 98.8% (means ± 2.5 SD) of the Gaussian distribution when the actual stimulation frequency was limited between 0 and 10 Hz. The variance of the GWN signal is 4 Hz^2. In contrast, the 0–10 Hz binary white noise used in the present study has a variance of 25 Hz^2. Hence, the binary white noise has a merit of increasing the input variance over the GWN when the stimulation frequency is limited between 0 and 10 Hz. Increasing the

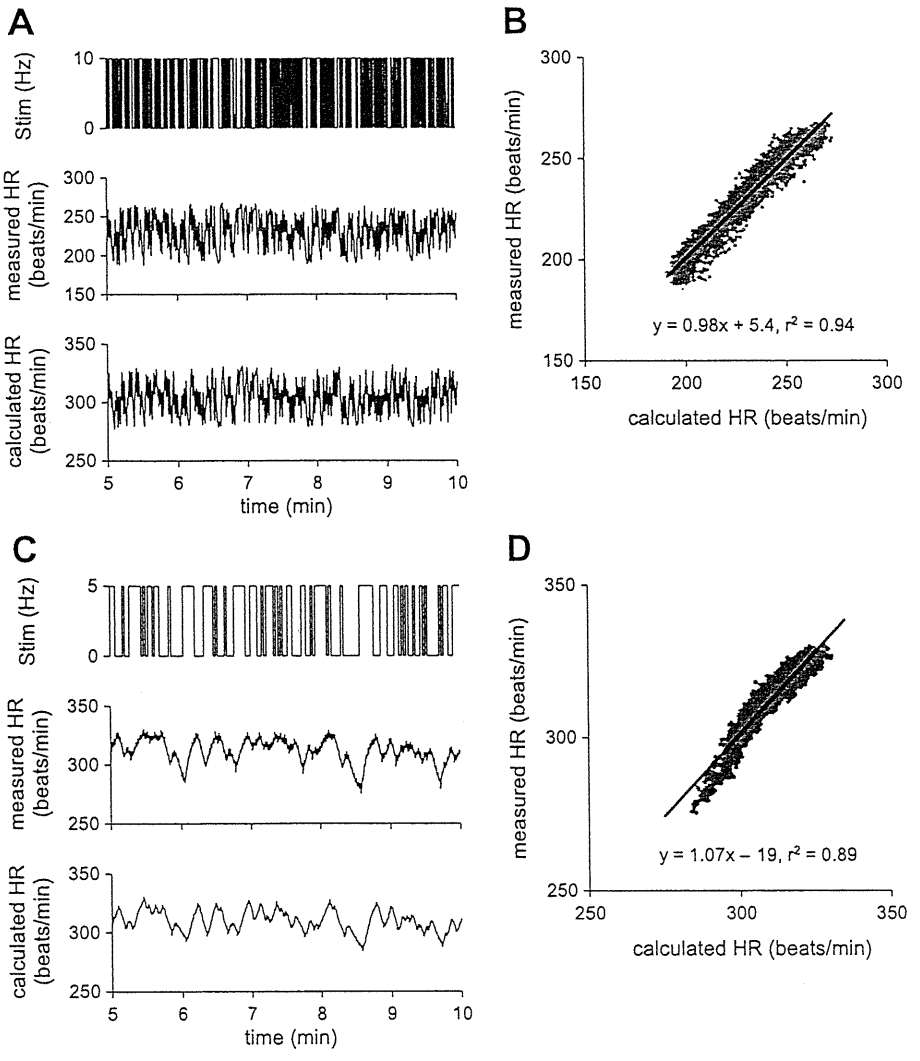

Fig. 5. *A*: data showing vagal stimulation (Stim), measured HR, and calculated HR based on the identified vagal transfer function of this animal. Time axis indicates the minutes after the initiation of random vagal stimulation (continuation of Fig. 1*A*). *B*: scatter plot between measured and calculated HR values. A solid line indicates a liner regression line. *C*: data showing sympathetic stimulation (Stim), measured HR, and calculated HR based on the identified sympathetic transfer function of this animal. Time axis indicates the minutes after the initiation of random sympathetic stimulation (continuation of Fig. 3*A*). *D*: scatter plot between measured and calculated HR values. A solid line indicates a linear regression line.

input variance is effective to increase the signal-to-noise ratio in the output signal and to improve the estimation of the transfer function.

In an earlier study on the transfer function analysis, Berger et al. (3) demonstrated that the roll-off of the vagal transfer function was gentle (i.e., the corner frequency was high) at high mean stimulatory rates and became more abrupt (i.e., the corner frequency was lower) with lower mean stimulatory rates. Although they attributed the difference in the roll-off characteristics to the difference in mean stimulatory rates, because they set the variance of input signal at ~1/4 of the mean stimulatory rates, which of the mean stimulatory rates or the input variance contributed to the determination of corner frequency seems inconclusive. Because there was no significant difference in the corner frequency between the vagal transfer functions estimated by GWNs of 5 ± 2 Hz and 10 ± 2 Hz (means ± SD) in a previous study from our laboratory (29), we speculate that the difference in the input variance rather than the mean stimulation frequency might have caused the different values of the corner frequency between the previous and the present results. This speculation requires further verification in future.

GRANTS

This study was supported by a Health and Labour Sciences Research Grant for Research on Advanced Medical Technology; a Health and Labour Sciences Research Grant for Research on Medical Devices for Analyzing, Supporting, and Substituting the Function of the Human Body; Health and Labour Sciences Research Grants H18-Iryo-Ippan-023, H18-Nano-Ippan-003, and H19-Nano-Ippan-009 from the Ministry of Health, Labour and Welfare of Japan; and the Industrial Technology Research Grant Program from the New Energy and Industrial Technology Development Organization of Japan.

REFERENCES

1. **Akselrod S, Gordon D, Ubel FA, Shannon DC, Berger AC, Cohen RJ.** Power spectrum analysis of heart rate fluctuation: a quantitative probe of beat-to-beat cardiovascular control. *Science* 213: 220–222, 1981.
2. **Andrews PL, Dutia MB, Harris PJ.** Angiotensin II does not inhibit vagally-induced bradycardia or gastric contractions in the anaesthetized ferret. *Br J Pharmacol* 82: 833–837, 1984.
3. **Berger RD, Saul JP, Cohen RJ.** Transfer function analysis of autonomic regulation. I. Canine atrial rate response. *Am J Physiol Heart Circ Physiol* 256: H142–H152, 1989.
4. **Brigham EO.** FFT transform applications. In: *The Fast Fourier Transform and Its Applications*. Englewood Cliffs, NJ: Prentice-Hall, 1988, p. 167–203.
5. **Brooks VL.** Chronic infusion of angiotensin II resets baroreflex control of heart rate by an arterial pressure-independent mechanism. *Hypertension* 26: 420–424, 1995.
6. **Castillo-Hernandez JR, Rubio-Gayosso I, Sada-Ovalle I, Garcia-Vazquez A, Ceballos G, Rubio R.** Intracoronary angiotensin II causes inotropic and vascular effects via different paracrine mechanisms. *Vascul Pharmacol* 41: 147–158, 2004.
7. **Dendorfer A, Thornagel A, Raasch W, Grisk O, Tempel K, Dominiak P.** Angiotensin II induces catecholamine release by direct ganglionic excitation. *Hypertension* 40: 348–354, 2002.
8. **DiBona GF.** Physiology in perspective: the wisdom of the body. Neural control of the kidney. *Am J Physiol Regul Integr Comp Physiol* 289: R633–R641, 2005.
9. **Diz DI, Averill DB.** Angiotensin II/autonomic interactions. In: *Primer on the Autonomic Nervous System*, edited by Robertson D, Biaggioni I, Burnstock G, and Low PA. San Diego: Elsevier Academic Press, 2004, p. 168–171.
10. **Farrell DM, Wei CC, Tallaj J, Ardell JL, Armour JA, Hageman GR, Bradley WE, Dell'Italia LJ.** Angiotensin II modulates catecholamine release into interstitial fluid of canine myocardium in vivo. *Am J Physiol Heart Circ Physiol* 281: H813–H822, 2001.
11. **Glantz SA.** *Primer of Biostatistics* (5th ed.). New York: McGraw-Hill, 2002.
12. **Jackson EK.** Autonomic control of the kidney. In: *Primer on the Autonomic Nervous System*, edited by Robertson D, Biaggioni I, Burnstock G, and Low PA. San Diego: Elsevier Academic Press, 2004, p. 157–161.
13. **Kashihara K, Takahashi Y, Chatani K, Kawada T, Zheng C, Li M, Sugimachi M, Sunagawa K.** Intravenous angiotensin II does not affect dynamic baroreflex characteristics of the neural or peripheral arc. *Jpn J Physiol* 53: 135–143, 2003.
14. **Kawada T, Ikeda Y, Sugimachi M, Shishido T, Kawaguchi O, Yamazaki T, Alexander J Jr, Sunagawa K.** Bidirectional augmentation of heart rate regulation by autonomic nervous system in rabbits. *Am J Physiol Heart Circ Physiol* 271: H288–H295, 1996.
15. **Kawada T, Miyamoto T, Miyoshi Y, Yamaguchi S, Tanabe Y, Kamiya A, Shishido T, Sugimachi M.** Sympathetic neural regulation of heart rate is robust against high plasma catecholamine. *J Physiol Sci* 56: 235–245, 2006.
16. **Kawada T, Uemura K, Kashihara K, Jin Y, Li M, Zheng C, Sugimachi M, Sunagawa K.** Uniformity in dynamic baroreflex regulation of left and right cardiac sympathetic nerve activities. *Am J Physiol Regul Integr Comp Physiol* 284: R1506–R1512, 2003.
17. **Kawada T, Yamazaki T, Akiyama T, Li M, Zheng C, Shishido T, Mori H, Sugimachi M.** Angiotensin II attenuates myocardial interstitial acetylcholine release in response to vagal stimulation. *Am J Physiol Heart Circ Physiol* 293: H2516–H2522, 2007.
18. **Khan MH, Sinoway LI.** Congestive heart failure. In: *Primer on the Autonomic Nervous System*, edited by Robertson D, Biaggioni I, Burnstock G, and Low PA. San Diego: Elsevier Academic Press, 2004, p. 247–248.
19. **Lameris TW, de Zeeuw S, Duncker DJ, Alberts G, Boomsma F, Verdouw PD, van den Meiracker AH.** Exogenous angiotensin II does not facilitate norepinephrine release in the heart. *Hypertension* 40: 491–497, 2002.
20. **Levy MN.** Sympathetic-parasympathetic interactions in the heart. *Circ Res* 29: 437–445, 1971.
21. **Li M, Zheng C, Sato T, Kawada T, Sugimachi M, Sunagawa K.** Vagal nerve stimulation markedly improves long-term survival after chronic heart failure in rats. *Circulation* 109: 120–124, 2004.
22. **Lokhandwala MF, Amelang E, Buckley JP.** Facilitation of cardiac sympathetic function by angiotensin II: role of presynaptic angiotensin receptors. *Eur J Pharmacol* 52: 405–409, 1978.
23. **Marmarelis PZ, Marmarelis VZ.** The white noise method in system identification. In: *Analysis of Physiological Systems*. New York: Plenum, 1978, p. 131–221.
24. **Miyamoto T, Kawada T, Takaki H, Inagaki M, Yanagiya Y, Jin Y, Sugimachi M, Sunagawa K.** High plasma norepinephrine attenuates the dynamic heart rate response to vagal stimulation. *Am J Physiol Heart Circ Physiol* 284: H2412–H2418, 2003.
25. **Miyamoto T, Kawada T, Yanagiya Y, Inagaki M, Takaki H, Sugimachi M, Sunagawa K.** Cardiac sympathetic nerve stimulation does not attenuate dynamic vagal control of heart rate via α-adrenergic mechanism. *Am J Physiol Heart Circ Physiol* 287: H860–H865, 2004.
26. **Mizuno M, Kamiya A, Kawada T, Miyamoto T, Shimizu S, Sugimachi M.** Muscarinic potassium channels augment dynamic and static heart rate responses to vagal stimulation. *Am J Physiol Heart Circ Physiol* 293: H1564–H1570, 2007.
27. **Nakahara T, Kawada T, Sugimachi M, Miyano H, Sato T, Shishido T, Yoshimura R, Miyashita H, Inagaki M, Alexander J Jr, Sunagawa K.** Accumulation of cAMP augments dynamic vagal control of heart rate. *Am J Physiol Heart Circ Physiol* 275: H562–H567, 1998.
28. **Nakahara T, Kawada T, Sugimachi M, Miyano H, Sato T, Shishido T, Yoshimura R, Miyashita H, Inagaki M, Alexander J Jr, Sunagawa K.** Neuronal uptake affects dynamic characteristics of heart rate response to sympathetic stimulation. *Am J Physiol Regul Integr Comp Physiol* 277: R140–R146, 1999.
29. **Nakahara T, Kawada T, Sugimachi M, Miyano H, Sato T, Shishido T, Yoshimura R, Miyashita H, Sunagawa K.** Cholinesterase affects dynamic transduction properties from vagal stimulation to heart rate. *Am J Physiol Regul Integr Comp Physiol* 275: R541–R547, 1998.
30. **Peach MJ, Bumpus FM, Khairallah PA.** Inhibition of norepinephrine uptake in hearts by angiotensin II and analogs. *J Pharmacol Exp Ther* 167: 291–299, 1969.
31. **Potter EK.** Angiotensin inhibits action of vagus nerve at the heart. *Br J Pharmacol* 75: 9–11, 1982.
32. **Reid IA, Chou L.** Analysis of the action of angiotensin II on the baroreflex control of heart rate in conscious rabbits. *Endocrinology* 126: 2749–2756, 1990.
33. **Starke K.** Action of angiotensin on uptake, release and metabolism of ^{14}C-noradrenaline by isolated rabbit hearts. *Eur J Pharmacol* 14: 112–123, 1971.
34. **Task Force of the European Society of Cardiology, the North American Society of Pacing and Electrophysiology.** Heart rate variability: standards of measurement, physiological interpretation and clinical use. *Circulation* 93: 1043–1065, 1996.
35. **Zimmerman BG, Sybertz EJ, Wong PC.** Interaction between sympathetic and renin-angiotensin system. *J Hypertens* 2: 581–587, 1984.

Journal of the American College of Cardiology
© 2009 by the American College of Cardiology Foundation
Published by Elsevier Inc.

Vol. 53, No. 8, 2009
ISSN 0735-1097/09/$36.00
doi:10.1016/j.jacc.2008.11.014

PRE-CLINICAL RESEARCH

Prolonged Targeting of Ischemic/Reperfused Myocardium by Liposomal Adenosine Augments Cardioprotection in Rats

Hiroyuki Takahama, MD,*†‡ Tetsuo Minamino, MD, PHD,§ Hiroshi Asanuma, MD, PHD,† Masashi Fujita, MD, PHD,§ Tomohiro Asai, PHD,¶ Masakatsu Wakeno, MD, PHD,*†‡ Hideyuki Sasaki, MD,*†‡ Hiroshi Kikuchi, PHD,# Kouichi Hashimoto,** Naoto Oku, PHD,¶ Masanori Asakura, MD, PHD,† Jiyoong Kim, MD,† Seiji Takashima, MD, PHD,§ Kazuo Komamura, MD, PHD,‖ Masaru Sugimachi, MD, PHD,‖ Naoki Mochizuki, MD, PHD,*‡ Masafumi Kitakaze, MD, PHD, FACC†

Osaka, Shizuoka, and Tokyo, Japan

Objectives The purpose of this study was to investigate whether liposomal adenosine has stronger cardioprotective effects and fewer side effects than free adenosine.

Background Liposomes are nanoparticles that can deliver various agents to target tissues and delay degradation of these agents. Liposomes coated with polyethylene glycol (PEG) prolong the residence time of drugs in the blood. Although adenosine reduces the myocardial infarct (MI) size in clinical trials, it also causes hypotension and bradycardia.

Methods We prepared PEGylated liposomal adenosine (mean diameter 134 ± 21 nm) by the hydration method. In rats, we evaluated the myocardial accumulation of liposomes and MI size at 3 h after 30 min of ischemia followed by reperfusion.

Results The electron microscopy and ex vivo bioluminescence imaging showed the specific accumulation of liposomes in ischemic/reperfused myocardium. Investigation of radioisotope-labeled adenosine encapsulated in PEGylated liposomes revealed a prolonged blood residence time. An intravenous infusion of PEGylated liposomal adenosine (450 μg/kg/min) had a weaker effect on blood pressure and heart rate than the corresponding dose of free adenosine. An intravenous infusion of PEGylated liposomal adenosine (450 μg/kg/min) for 10 min from 5 min before the onset of reperfusion significantly reduced MI size (29.5 ± 6.5%) compared with an infusion of saline (53.2 ± 3.5%, $p < 0.05$). The antagonist of adenosine A_1, A_{2a}, A_{2b}, or A_3 subtype receptor blocked cardioprotection observed in the PEGylated liposomal adenosine-treated group.

Conclusions An infusion as PEGylated liposomes augmented the cardioprotective effects of adenosine against ischemia/reperfusion injury and reduced its unfavorable hemodynamic effects. Liposomes are promising for developing new treatments for acute MI. (J Am Coll Cardiol 2009;53:709–17) © 2009 by the American College of Cardiology Foundation

Liposomes are now widely used for drug delivery in cancer treatment to target specific organs actively or passively and to prevent the degradation of chemotherapy agents (1). However, the application of liposomes for cardiovascular diseases is still limited. In ischemic/reperfused myocardium,

See page 718

cellular permeability is enhanced and vascular endothelial integrity is disrupted (2,3), suggesting that nanoparticles

*From the Department of Molecular Imaging in Cardiovascular Medicine, Osaka University Graduate School of Medicine, Osaka, Japan; †Department of Cardiovascular Medicine, National Cardiovascular Center, Osaka, Japan; ‡Department of Structural Analysis, Research Institute, National Cardiovascular Center, Osaka, Japan; §Department of Cardiovascular Medicine, Osaka University Graduate School of Medicine, Osaka, Japan; ‖Department of Cardiovascular Dynamics, Research Institute, National Cardiovascular Center, Osaka, Japan; ¶Department of Medical Biochemistry, School of Pharmaceutical Sciences, University of Shizuoka, Shizuoka, Japan; #Daiichi Pharmaceutical Co., Tokyo, Japan; and the **Daiichi-Sankyo Pharmaceutical Co., Tokyo, Japan. Supported by a grant for Scientific Research and a grant for the Advancement of Medical Equipment from the Japanese Ministry of Health, Labor, and Welfare, as well as a grant from the Japan Cardiovascular Research Foundation.

Manuscript received September 4, 2008; revised manuscript received October 21, 2008, accepted November 3, 2008.

JACC Vol. 53, No. 8, 2009
February 24, 2009:709–17

Abbreviations and Acronyms

8-SPT = 8-(p-sulfophenyl) theophylline
EM = electron microscopy
MI = myocardial infarction
PEG = polyethylene glycol
RI = radioisotope
TTC = triphenyltetrazolium chloride

such as liposomes may be a promising drug delivery system for targeting damaged myocardium with cardioprotective agents. Additionally, coating liposomes with polyethylene glycol (PEG) prolongs their residence time in the circulation (1). Because enhanced microvascular permeability persists for at least 48 h after the occurrence of myocardial infarction (MI) (2), drugs delivered in PEGylated liposomes should be able to display their maximum beneficial effects on myocardial damage after MI.

Adenosine has multiple physiological functions that are mediated via the adenosine A_1, A_{2a}, A_{2b}, and A_3 receptors (4,5). Although large-scale clinical trials suggested the potential value of adenosine therapy for patients with acute MI (6,7), this agent has an extremely short half-life (1 to 2 s) and causes hypotension and bradycardia because of vasodilatory and negative chronotropic effects (4). Because a high dose of adenosine is required to exert cardioprotective effects, it is difficult to use clinically because of the associated hemodynamic consequences. Therefore, we hypothesized that adenosine encapsulated in PEGylated liposomes would cause less hemodynamic disturbance and might also specifically accumulate in ischemic/reperfused myocardium, leading to augmented cardioprotective effects. To test this hypothesis, we created PEGylated liposomal adenosine by the hydration method and investigated: 1) whether liposomal adenosine accumulated in ischemic/reperfused myocardium and prolonged blood residence time; 2) whether liposomal adenosine caused less severe hypotension and bradycardia than free adenosine; and 3) which adenosine receptor subtype was involved in mediating the cardioprotective effects of liposomal adenosine against ischemia/reperfusion injury.

Methods

Materials. The materials for preparing PEGylated liposomes, including hydrogenated soy phosphatidyl choline (HSPC), 1,2-distearoyl-sn-glycero-3-phosphoethanolamine-n-[methoxy (polyethylene glycol)-2000] (DSPE-PEG2000), and cholesterol were obtained from Nissei Oil Co., Ltd. (Tokyo, Japan) and Wako Pure Chemical Co., Ltd. (Osaka, Japan). [^{3}H]-adenosine was purchased from Daiichi Pure Chemicals Co., Ltd. (Tokyo, Japan). Other materials were obtained from Sigma (St. Louis, Missouri), including 8-(*p*-sulfophenyl)theophylline (8-SPT; a nonselective adenosine receptor antagonist), 1,3-diethyl-8-phenylxanthine (DPCPX; a selective adenosine A_1 receptor antagonist), 5-amino-7-(phenylethyl)-2-(2-furyl)-pyrazolo[4,3-e]-1,2,4-triazolo[1,5-c] pyrimidine (SCH58261; a selective adenosine A_{2a} receptor antagonist), 8-[4-[((4-cyanophenyl)carbamoylmethyl) oxy]phenyl]-1, 3-di(n-propyl)xanthine (MRS1754; a selective adenosine A_{2b} receptor antagonist), and 5-propyl-2-ethyl-4-propyl-3-(ethylsulfanylcarbonyl)-6-phenylpyridine-5-carboxylate (MRS1523, a selective adenosine A_3 receptor antagonist).

Animals. Male Wistar rats (9 weeks old and weighing 250 to 310 g, Japan Animals, Osaka, Japan) were used. The animal experiments were approved by the National Cardiovascular Center Research Committee and were performed according to institutional guidelines.

Preparation of PEGylated liposomes. The PEGylated liposomes were prepared by the hydration method. Briefly, adenosine was added to the lipid solution. After mixture of lipid and adenosine, DSPE-PEG2000 was added and incubated. The final composition of PEGylated liposomes was HSPC:cholesterol:DSPE-PEG2000 = 6.0:4.0:0.3 (molar ratio). After ultracentrifugation several times, the pellet of liposomal adenosine was resuspended in sodium lactate at each required concentration for use in the experimental protocols. Some samples of final liposomal adenosine were disrupted by dilution with 50% methanol (1.5 ml per 30-μl of liposomes). After 10 min of ultracentrifugation, the concentration of adenosine in the supernatant was measured by high-performance liquid chromatography.

To prepare fluorescent-labeled liposomes, 0.5 mol% tetramethylrhodamine isothiocyanate (rhodamine) was added to the lipid mixture. To prepare radioisotope (RI)-labeled adenosine encapsulated in liposomes, [^{3}H]-radiolabeled adenosine (Daiichi Pure Chemicals, Tokyo, Japan) was diluted with free adenosine and was encapsulated in liposomes as described above.

Characterization of PEGylated liposomal adenosine. The characterization of the liposomes was performed by the dynamic scatter analysis (Zetasizer Nano ZS, Malvern, Worcestershire, United Kingdom). The analyses were performed 10 times per sample, and results represented analyses of 4 independent experiments.

Experimental protocols. PROTOCOL 1: EFFECTS OF PEGYLATED LIPOSOMAL ADENOSINE ON HEMODYNAMICS IN RATS. Rats were anesthetized with intraperitoneal sodium pentobarbital (50 mg/kg). Catheters were advanced into a femoral artery and vein for the measurement of systemic blood pressure and infusion of drugs, respectively. Both blood pressure and heart rate were monitored continuously during the study using a Power Lab (AD Instruments, Castle Hill, Australia). After hemodynamics became stable, we intravenously administered empty PEGylated liposomes (n = 8), free adenosine (n = 8), or PEGylated liposomal adenosine (n = 8) for 10 min. Either PEGylated liposomal or free adenosine was infused at an initial dose of 225 μg/kg/min (0.1 ml/min) for 10 min. After a 5-min interval, either PEGylated liposomal adenosine or free adenosine was infused at 450 μg/kg/min (0.1 ml/min) for 10 min. In the same manner, PEGylated liposomal adenosine or free adenosine was then infused at 900 μg/kg/min (0.1 ml/min).

PROTOCOL 2: EFFECTS OF PEGYLATED LIPOSOMAL ADENOSINE ON INFARCT SIZE IN RATS. The MI was induced by transient ligation of the left coronary artery as described previously (8). In the first series of experiments, to examine the dose-dependent effects of liposomal adenosine on MI size, PEGylated liposomal adenosine was infused intravenously at 50, 150, or 450 μg/kg/min for a 10-min period starting from 5 min before the onset of reperfusion. In the second series of experiments, to determine the adenosine receptor subtype involved in cardioprotective effects by the liposomal adenosine, the antagonist of adenosine subtype receptor was intravenously injected as a bolus followed by the infusion of liposomal adenosine for 10 min. The MI size was evaluated at 3 h after the start of reperfusion. The doses of adenosine receptor subtype antagonists were determined according to the previous reports (9–11).

Measurement of infarct size. At 3 h after the onset of reperfusion, the area at risk and the infarcted area were determined by Evans blue and triphenyltetrazolium chloride (TTC) staining, respectively, as previously described (8). Infarct size was calculated as [infarcted area/area at risk] × 100(%) in a blind manner. The area at risk was composed of border (TTC staining) and infarcted (TTC nonstaining) areas.

Electron microscopy (EM). Myocardial samples for EM were obtained from the central and peripheral areas in ischemic/reperfused myocardium, which roughly corresponded to the infarcted and border areas, respectively, after the left coronary artery was occluded for 30 min of ischemia followed by 3 h of reperfusion. Samples were prepared as previously reported (12). Liposomes, whose major membrane component is unsaturated phospholipids, were visualized as homogenous dark dots with a diameter of 100 to 150 nm (13).

Accumulation of fluorescent-labeled PEGylated liposomes in ischemic/reperfused myocardium. Unlabeled or fluorescent-labeled PEGylated liposomes were infused intravenously at a dose of 0.1 ml/min as liposomal adenosine was infused in protocol 2. At 3 h after reperfusion, hearts were quickly removed and cut into 4 sections parallel to the axis from base to apex. Then ex vivo bioluminescence imaging was performed with an Olympus OV 100 imaging system (Olympus, Tokyo, Japan) and signals were quantified using WASABI quantitative software (Hamamatsu Photonics K.K., Shizuoka, Japan). Fluorescent intensity in the region of interest was measured as previously reported (14). Control intensity indicated the fluorescent intensity in the nonischemic area of the individual rat.

Time-course changes of free and PEGylated liposomal RI-labeled adenosine in plasma and myocardium. Free or PEGylated liposomal [^{3}H]-adenosine (83 kBq per rat) was infused intravenously at a dose of 0.1 ml/min as liposomal adenosine was infused in protocol 2. At the time indicated, rat hearts were harvested for counting of radioactivity (LSC-3100, Aloka Co., Tokyo, Japan). Results are expressed as a percentage of the injected dose per 1 ml of blood or 1 g of wet tissue weight.

Statistical analysis. The parameters of the liposomes were expressed as the average ± SD, whereas other data were expressed as the average ± SEM. Comparison of time-course changes in hemodynamic parameters between groups was performed by 2-way repeated-measures analysis of variance (ANOVA) followed by a post-hoc Bonferroni test. For comparison of RI activity between groups, statistical analysis was done with the Mann-Whitney *U* test. To address the differences in infarct size among groups, we performed a nonparametric (Kruskal-Wallis) test followed by evaluation with the Mann-Whitney *U* test. Resulting p values were corrected according to the Bonferroni method. To compare parameters of liposomes, an unpaired *t* test was performed. In all analyses, $p < 0.05$ was considered to indicate statistical significance.

Results

Characterization of liposomes by dynamic light scatter analysis. The dynamic light scatter analysis showed no significant difference in mean diameter, polydispersity index, or zeta-potential distribution between empty and adenosine-loaded PEGylated liposomes (Table 1).

Liposomes in ischemic/reperfused myocardium. The EM revealed the intact vascular endothelial cells and cardiomyocytes in the nonischemic myocardium (Figs. 1A and 1B). There were no homogenous dark dots indicating liposomes in the nonischemic myocardium of rats that received either saline (Fig. 1A) or liposomes (Fig. 1B). In the border area, many homogenous dark dots indicating liposomes were accumulated in rats that received liposomes, but not saline (Figs. 1C and 1D). In this area, significant structural damage was not observed in endothelium, but slight swelling of mitochondria was often observed. In the infarcted area, numerous liposomes were detected in rats that received liposomes, but not saline (Figs. 1E and 1F). In this area, the disrupted endothelial integrity and marked swelling of mitochondria were often observed.

Table 1 Characterization of Liposomes by Dynamic Light Scatter Analysis

	Mean Diameter (nm)	Polydispersity Index	Zeta Potential (mV)
PEGylated liposomes (empty liposomes)	126 ± 12	0.035 ± 0.003	−1.7 ± 0.4
PEGylated liposomal adenosine	134 ± 21	0.094 ± 0.002	−2.3 ± 1.1

Results represented analysis of 4 independent experiments. Values are expressed as mean ± SD.
PEG = polyethylene glycol.

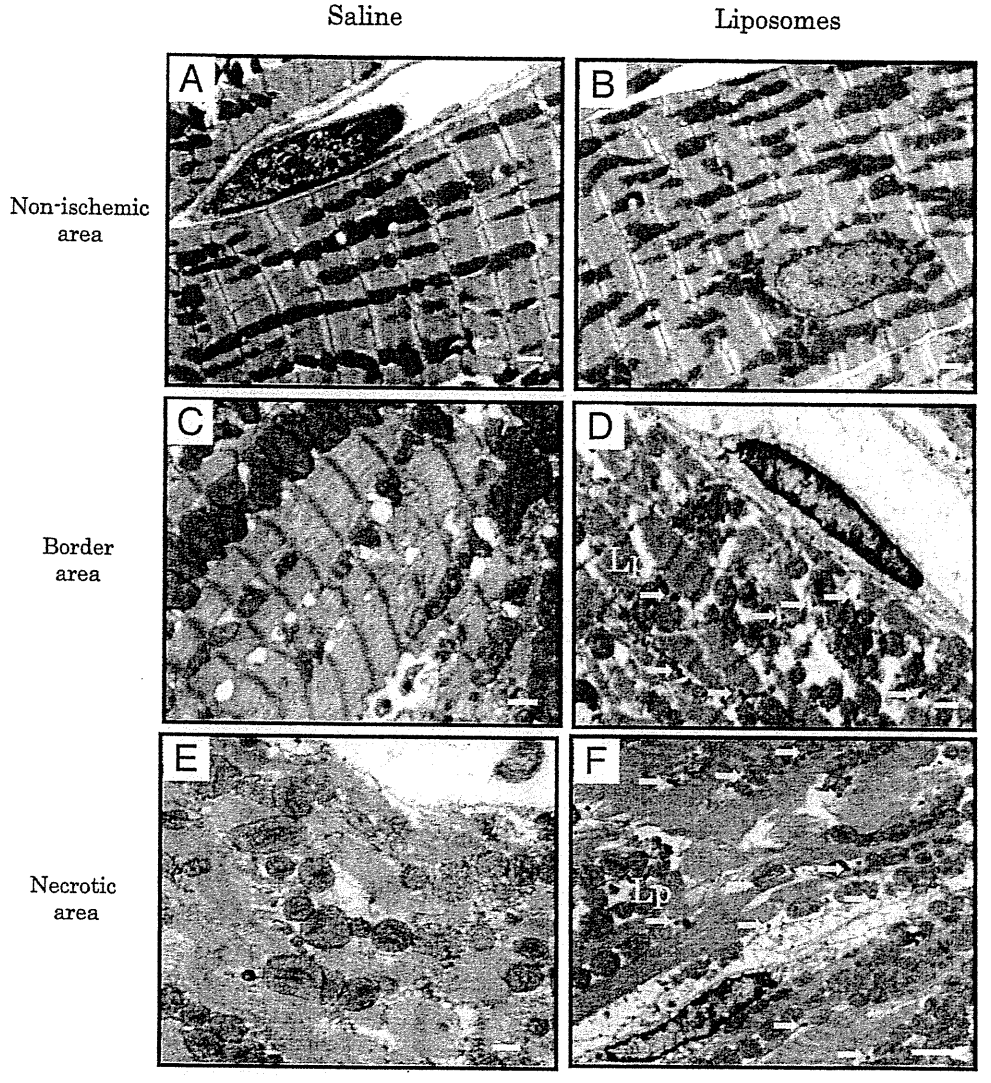

Figure 1 **Liposomes in Ischemic/Reperfused Myocardium**

(A, B) Representative electron micrographs of the nonischemic area in rats that received saline **(A)** or liposomes (Lp) **(B)**. **(C, D)** Representative electron micrographs of border area at 3 h after myocardial infarction (MI). Many **dark dots** accumulated in this area in the rat that received liposomes but not saline. **(E, F)** Representative electron micrographs of infarcted areas at 3 h after MI. Numerous **dark dots** accumulated in this area in the rat that received liposomes but not saline. Scale bars represent 1 μm.

Fluorescent-labeled PEGylated liposomes in ischemic/reperfused myocardium. Quantitative analysis by bioluminescence ex vivo bioluminescene imaging revealed that the target to control fluorescent intensity ratio was higher in the border (noninfarcted area at risk) as well as infarcted areas compared with a nonischemic one, suggesting that fluorescent-labeled liposomes were accumulated in the border as well as infarcted areas. Since there was no high-intensity area when unlabeled liposomes were infused, it was suggested that this was not a nonspecific phenomenon to MI by the ex vivo bioluminescence imaging system (Fig. 2). The Evans blue staining was unrelated to the fluorescence intensity (data not shown).

Plasma radioactivity of RI-labeled adenosine was markedly higher in the PEGylated liposomal adenosine group at 10 min and 3 h after the intravenous infusion than in the free adenosine group (Fig. 3A). Encapsulation within PEGylated liposomes also augmented the accumulation of adenosine in ischemic/reperfused myocardium compared with that of free adenosine (Fig. 3B).

Hemodynamic effects of PEGylated liposomal adenosine. Baseline hemodynamic parameters did not differ among the groups. An intravenous infusion of free adenosine at doses of 225, 450, and 900 μg/kg/min decreased the mean blood pressure by 14.8%, 25.4%, and 33.7%, respectively, compared with the effect of empty PEGylated lipo-

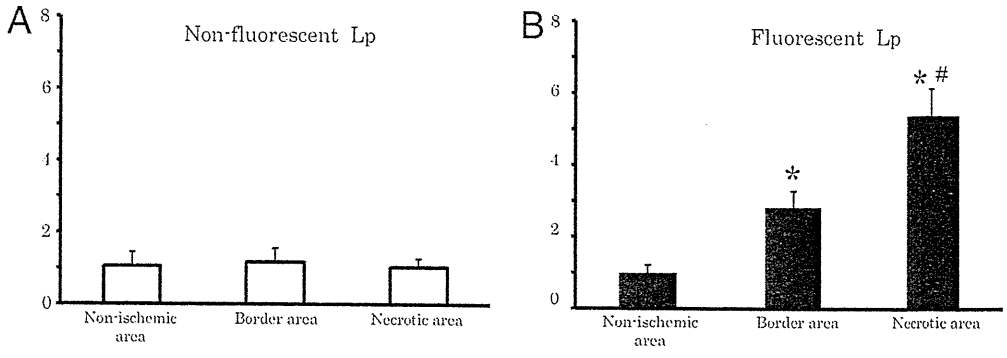

Figure 2 **Detection of Fluorescence-Labeled PEGylated Liposomes in Ischemic/Reperfused Myocardium**

Quantitative analysis of target-to-control fluorescent intensity ratio for each area in rats (n = 3 each group) that received nonfluorescent **(A)** or fluorescent **(B)** liposomes. The values of bioluminescence signals in the border and infarcted areas were expressed as the fold to that of the each nonischemic area. Values are expressed as the mean ± SEM (error bars). *p < 0.05 versus nonischemic areas. #p < 0.05 versus border areas.

somes. In contrast, the intravenous infusion of PEGylated liposomal adenosine at a dose of either 225 or 450 μg/kg/min did not significantly alter mean blood pressure (Fig. 4). Changes of the heart rate after infusion of PEGylated liposomal adenosine or free adenosine were similar to those observed for mean blood pressure (Fig. 4).

Effects of PEGylated liposomal adenosine on MI size. Baseline hemodynamic parameters were similar among all of the groups (Table 2). Intravenous infusion of free adenosine for 10 min reduced both the blood pressure and the heart rate, although these parameters returned to baseline within 5 min of ceasing infusion (Table 2). In contrast, hemodynamic parameters of the other groups were not altered (Table 2). The area at risk in the control group (61 ± 3%) did not differ compared with those of other groups that received liposomal adenosine. Intravenous infusion of PEGylated liposomal adenosine caused a dose-dependent decrease of MI size compared with that in the control group, whereas intravenous infusion of empty PEGylated liposomes or free adenosine did not (Fig. 5B).

The bolus injection of adenosine receptor antagonist did not alter the hemodynamic parameters (Table 3). The area at risk in the liposomal adenosine group (58 ± 3%) did not differ compared with those of other groups that received adenosine receptor antagonist. Infusion of 8-SPT, a nonspecific adenosine receptor antagonist, blunted the cardioprotective effect of liposomal adenosine (Fig. 6B). Furthermore, the infusion of the adenosine A_1, A_{2a}, A_{2b}, or A_3 receptor antagonist also blunted cardioprotective effects of liposomal adenosine (Fig. 6B). Infusion of 8-SPT alone did not significantly affect myocardial infarct size compared with the control (52 ± 5%, n = 4).

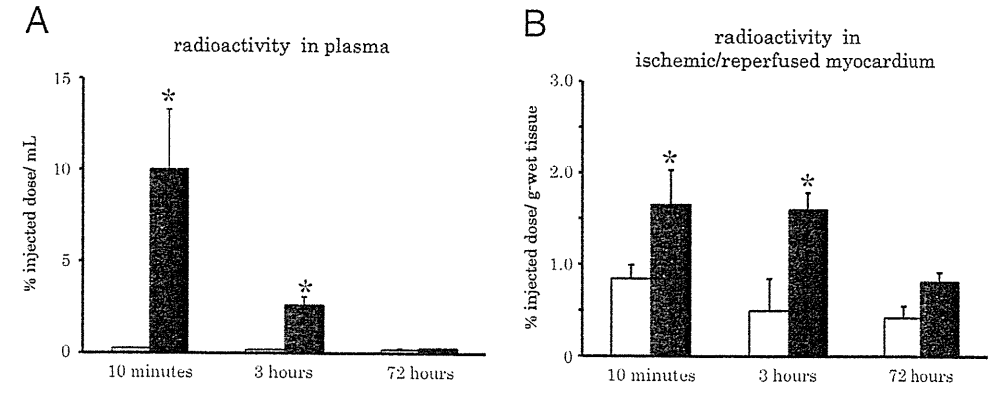

Figure 3 **Radioisotope-Labeled Adenosine in Plasma and Ischemic/Reperfused Myocardium**

(A) Changes in plasma radioactivity after infusion of radioisotope-labeled adenosine. **Solid and open bars** indicate the PEGylated liposomal adenosine and free adenosine groups, respectively (n = 4 each). In the PEGylated liposomal adenosine group, plasma radioactivity was markedly higher than in the free adenosine group. **(B)** Changes in radioactivity in ischemic/reperfused myocardium. **Solid and open bars** indicate the PEGylated liposomal adenosine and free adenosine groups, respectively (n = 4 each). In the PEGylated liposomal adenosine group, myocardial radioactivity was markedly higher than in the free adenosine group. Values are expressed as the mean ± SEM (error bars). *p < 0.05 versus the free adenosine group at the corresponding time.

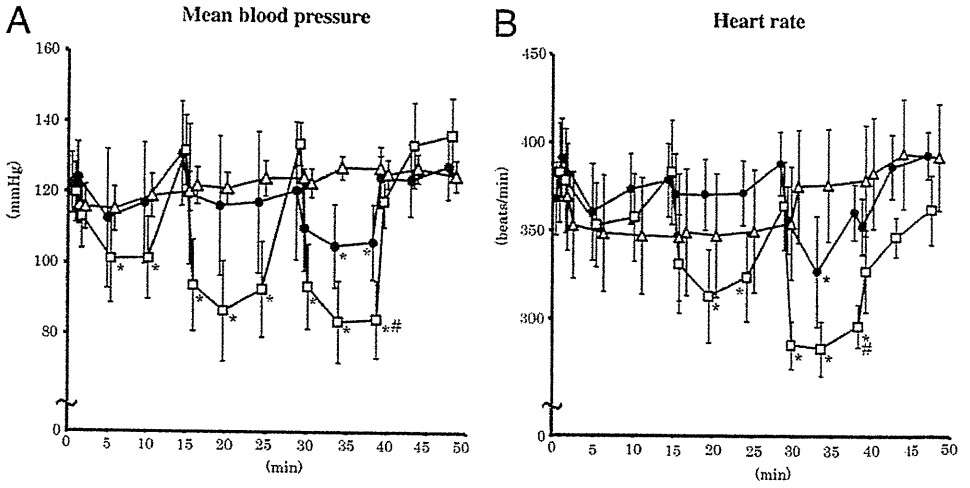

Figure 4 **Hemodynamic Effects of PEGylated Liposomal Adenosine**

Changes in the mean blood pressure **(A)** and heart rate **(B)** after intravenous infusion of various doses of empty PEGylated liposomes **(triangles)**, PEGylated liposomal adenosine **(circles)**, or free adenosine **(squares)** (n = 8 each). Values are expressed as the mean ± SEM. *p < 0.05 versus baseline at the corresponding group. #p < 0.05 versus PEGylated liposomes.

Discussion

In the present study, EM, bioluminescence ex vivo imaging, and fluorescent analysis revealed the accumulation of liposomes in the border (noninfarcted areas at risk) as well as infarcted ones, but not nonischemic myocardium, at 3 h after MI. These findings suggested that liposomes could specifically accumulate in ischemic/reperfused myocardium. Interestingly, EM revealed the existence of liposomes at sites where endothelial integrity was still morphologically maintained. Endothelial dysfunction such as enhanced permeability is induced by ischemic insult without morphological endothelial disruption (3,15). Enhanced permeability might lead to the accumulation of liposomes in the border as well as infarcted area, which will contribute to salvage the ischemic/reperfused myocardium. However, further investigation will be needed to determine the precise mechanism by which liposomes accumulate in ischemic/reperfused myocardium.

Analysis using RI-labeled adenosine encapsulated in liposomes revealed that plasma radioactivity was markedly higher in the PEGylated liposomal adenosine group compared with the free adenosine group. This indicates that encapsulation of adenosine by PEGylated liposomes considerably prolonged its residence time in the circulation and delayed its degradation. Consistent with the histological data, RI-labeled adenosine also showed preferential accumulation in ischemic/reperfused myocardium.

Table 2 **Effects of Liposomal Adenosine on Hemodynamic Parameters**

		Ischemia				Reperfusion	
	Baseline	0 min	15 min	25 min	30 min	5 min	10 min
Mean blood pressure (mm Hg)							
Saline	122 ± 5	102 ± 10	108 ± 7	107 ± 9	108 ± 7	105 ± 9	104 ± 9
Vehicle	127 ± 4	109 ± 8	108 ± 7	111 ± 9	111 ± 5	105 ± 5	103 ± 5
Free-Ado	124 ± 8	115 ± 8	111 ± 5	109 ± 4	66 ± 4*	62 ± 4*	112 ± 6
Lp-Ado 50 μg/kg/min	121 ± 5	106 ± 6	105 ± 6	110 ± 10	102 ± 6	101 ± 6	104 ± 4
Lp-Ado 150 μg/kg/min	122 ± 3	107 ± 6	107 ± 6	109 ± 11	105 ± 6	100 ± 6	103 ± 4
Lp-Ado 450 μg/kg/min	124 ± 3	104 ± 6	105 ± 6	107 ± 5	102 ± 6	99 ± 6	104 ± 4
Heart rate (beats/min)							
Saline	363 ± 22	366 ± 19	369 ± 14	413 ± 22	372 ± 12	372 ± 16	371 ± 14
Vehicle	363 ± 32	363 ± 6	383 ± 6	396 ± 25	367 ± 6	374 ± 7	372 ± 7
Free-Ado	360 ± 18	361 ± 17	384 ± 13	379 ± 18	305 ± 11*	293 ± 13*	356 ± 14
Lp-Ado 50 μg/kg/min	378 ± 19	386 ± 21	366 ± 12	376 ± 12	367 ± 19	369 ± 9	377 ± 17
Lp-Ado 150 μg/kg/min	388 ± 27	376 ± 20	371 ± 14	377 ± 13	378 ± 16	373 ± 16	369 ± 17
Lp-Ado 450 μg/kg/min	368 ± 17	376 ± 21	361 ± 13	386 ± 15	368 ± 15	363 ± 6	367 ± 7

Values are expressed as mean ± SEM. *p < 0.05 versus baseline.
Free-Ado = free adenosine; Lp-Ado = PEGylated liposomal adenosine; PEG = polyethylene glycol; vehicle = PEGylated liposomes.

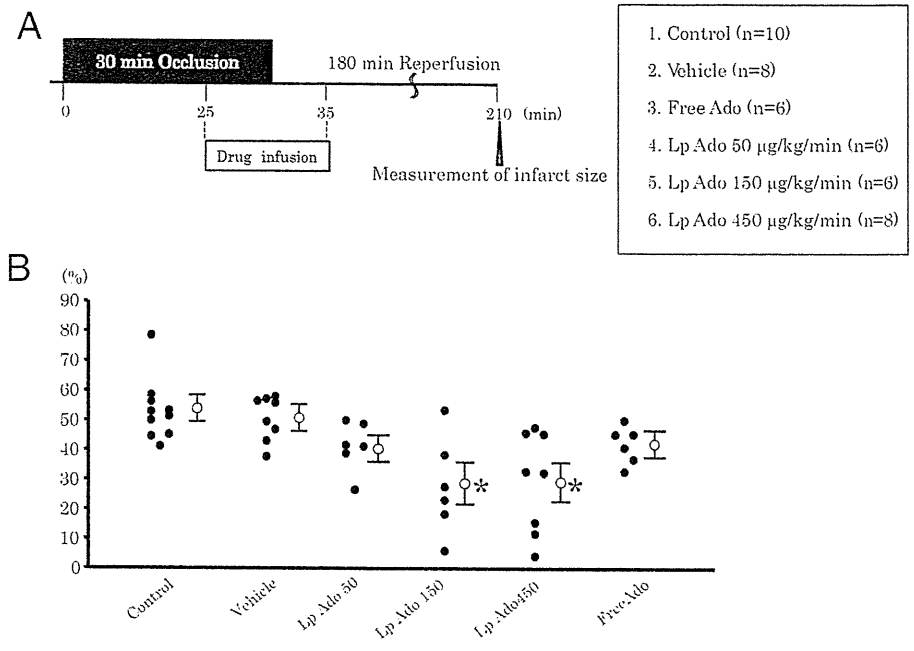

Figure 5 **Dose-Dependent Effects of PEGylated Liposomal Adenosine on Myocardial Infarct Size**

(A) Protocol showing the timing of infusion of PEGylated liposomal adenosine and of infarct size measurement. **(B)** Myocardial infarct size. Values are expressed as mean ± SEM (error bars). *p < 0.05 versus the control group. Free-Ado = free adenosine; Lp-Ado = PEGylated liposomal adenosine; Vehicle = PEGylated liposomes.

Furthermore, this study showed that PEGylated liposomal adenosine had a weaker effect on the blood pressure and heart rate than free adenosine. Thus, encapsulating adenosine in PEGylated liposomes attenuated its vasodilatory and negative chronotropic effects, presumably by reducing the amount of circulating free adenosine. However, the changes of hemodynamic parameters in this in vivo model suggested that significant release of adenosine from PEGylated liposomes would still occur if a large dose of liposomal adenosine (e.g., 900 μg/kg/min) were administered. Thus, further investigation of the in vivo pharmacodynamics of PEGylated liposomal adenosine is needed.

An intravenous infusion of PEGylated liposomal adenosine at the maximum dose that did not disturb hemodynamic parameters for 10 min before reperfusion reduced MI size in a dose-dependent manner, and this improvement was blocked by 8-SPT, a nonselective adenosine receptor antagonist. These findings suggest that adenosine released from liposomes acts via an adenosine receptor-dependent pathway. One possible mechanism by which PEGylated lipo-

Table 3 **Effects of Adenosine Receptor Antagonist on Hemodynamic Parameters**

		Ischemia				Reperfusion	
	Baseline	0 min	15 min	25 min	30 min	5 min	10 min
Mean blood pressure (mm Hg)							
Lp-Ado + 8SPT	120 ± 6	113 ± 4	112 ± 6	112 ± 5	107 ± 6	102 ± 8	109 ± 7
Lp-Ado + DPCPX	130 ± 6	105 ± 4	121 ± 4	100 ± 10	122 ± 6	120 ± 6	111 ± 4
Lp-Ado + SCH58261	132 ± 2	98 ± 12	99 ± 8	110 ± 8	118 ± 10	113 ± 10	109 ± 6
Lp-Ado + MRS1754	130 ± 3	95 ± 12	106 ± 8	105 ± 10	100 ± 10	96 ± 10	99 ± 7
Lp-Ado + MRS1523	130 ± 2	109 ± 8	104 ± 8	105 ± 9	100 ± 9	101 ± 10	104 ± 6
Heart rate (beats/min)							
Lp-Ado + 8SPT	404 ± 17	385 ± 10	374 ± 8	396 ± 8	389 ± 9	383 ± 8	385 ± 9
Lp-Ado + DPCPX	396 ± 24	380 ± 11	399 ± 9	398 ± 12	385 ± 9	382 ± 9	380 ± 7
Lp-Ado + SCH58261	393 ± 14	399 ± 15	381 ± 9	395 ± 15	376 ± 9	373 ± 9	385 ± 7
Lp-Ado + MRS1754	398 ± 14	392 ± 11	401 ± 9	379 ± 15	378 ± 9	374 ± 9	377 ± 7
Lp-Ado + MRS1523	396 ± 9	390 ± 11	390 ± 11	392 ± 10	373 ± 9	391 ± 7	388 ± 11

Values were expressed as mean ± SEM. *p < 0.05 versus baseline.
Lp-Ado = PEGylated liposomal adenosine; PEG = polyethylene glycol; Vehicle = PEGylated liposomes.

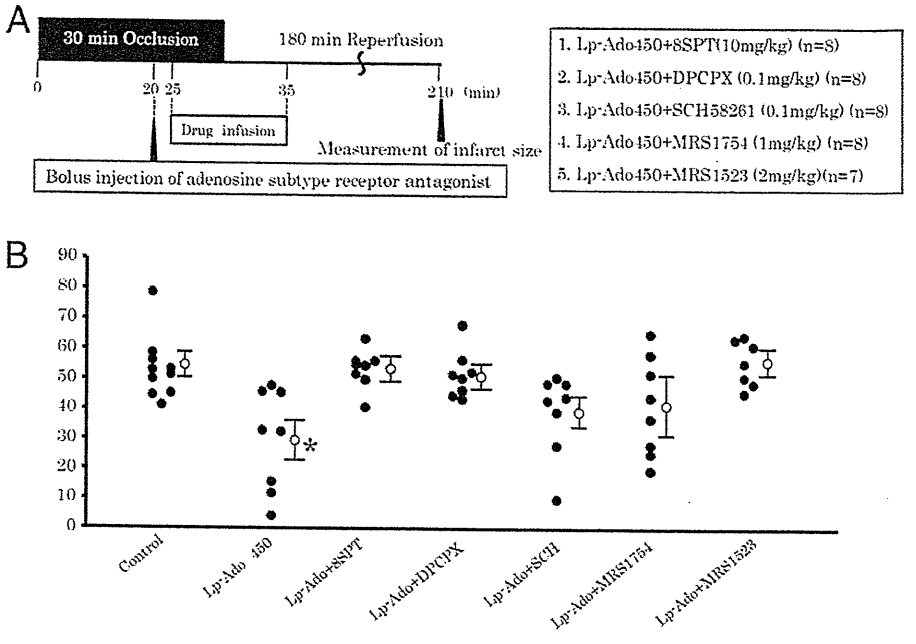

Figure 6 **Effects of Adenosine Receptor Antagonists on Myocardial Infarct Size**

(A) Protocol showing the timing of infusion of PEGylated liposomal adenosine and bolus injection adenosine receptor antagonists. (B) Myocardial infarct size. Values are expressed as the mean ± SEM (error bars). *$p < 0.05$ versus the control group. The abbreviations for adenosine antagonists were described in the text. Abbreviations as in Figure 5.

somes could augment cardioprotective effects of liposomal adenosine with minimum effects on hemodynamic parameters is the enhanced accumulation of PEGylated liposomal adenosine in ischemic/reperfused myocardium, which could augment various beneficial actions such as preventing calcium overload in the myocardium (5). The prolonged persistence of PEGylated liposomal adenosine would also increase its beneficial effect on ischemic/reperfused myocardium. Although continuous high-dose, long-term infusion of free adenosine was reported to reduce infarct size in rats (16), the present study did not confirm such a cardioprotective effect, probably because the total dose of free adenosine that we used was not high enough.

We found that myocardial infarct size in the group that received PEGylated liposomal adenosine with the antagonist of adenosine A_1, A_{2a}, A_{2b}, or A_3 subtype receptor was no different from the control group, indicating that every adenosine subtype receptor could possibly play a role in mediating cardioprotection by liposomal adenosine and that it was difficult to identify one particular subtype in the present study. Numerous studies reported that A_1, A_{2a}, A_{2b}, and A_3 receptors have been involved in cardioprotection against ischemia/reperfusion injury, and it remains controversial which adenosine subtype receptor is most responsible for cardioprotection (17–20). Furthermore, because the adenosine receptor antagonists used in the present study had some nonspecific effects, future investigation will be needed to examine the precise role of each adenosine receptor subtype using genetically engineered mice.

Because liposomal adenosine infused during reperfusion could reduce MI size, this agent could be a candidate for the adjunctive therapy of patients with acute MI. Importantly, adenosine is currently used for the diagnosis of ischemic heart disease and PEGylated liposomes are used to deliver anticancer agents (21). Thus, it should not be difficult to introduce PEGylated liposomal adenosine into clinical practice. Finally, PEGylated liposomes may provide a useful drug delivery system for targeting ischemic/reperfused myocardium with other agents.

Acknowledgments

The authors thank Akiko Ogai and Yoko Nakano for their excellent technical assistance; Motohide Takahama, Hiroyuki Hao, and Hatsue Ishibashi-Ueda for advice about the electron microscopy figure; and Syunichi Kuroda and Takashi Matsuzaki for assistance with bioluminescence imaging.

Reprint requests and correspondence: Dr. Tetsuo Minamino, Department of Cardiovascular Medicine, Osaka University Graduate School of Medicine, 2-2 Yamadaoka, Suita, Osaka 565-0871, Japan. E-mail: minamino@medone.med.osaka-u.ac.jp.

REFERENCES

1. Papahadjopoulos D, Allen TM, Gabizon A, et al. Sterically stabilized liposomes: improvements in pharmacokinetics and antitumor therapeutic efficacy. Proc Natl Acad Sci U S A 1991;24:11460–4.

2. Horwitz LD, Kaufman D, Keller MW, Kong Y. Time course of coronary endothelial healing after injury due to ischemia and reperfusion. Circulation 1994;90:2439–47.
3. Dauber IM, Van Benthuysen KM, McMurtry IF, et al. Functional coronary microvascular injury evident as increased permeability due to brief ischemia and reperfusion. Circ Res 1990;66:986–98.
4. Forman MB, Stone GW, Jackson EK. Role of adenosine as adjunctive therapy in acute myocardial infarction. Cardiovasc Drug Rev 2006;24: 116–47.
5. Mubagwa K, Flameng W. Adenosine, adenosine receptors and myocardial protection: an updated overview. Cardiovasc Res 2001;52:25–39.
6. Mahaffey KW, Pume JA, Barbagelata NA, et al. Adenosine as an adjunct to thrombolytic therapy for acute myocardial infarction: results of a multicenter, randomized, placebo-controlled trial: the Acute Myocardial Infarction STudy of ADenosine (AMISTAD) trial. J Am Coll Cardiol 1999;34:1711–20.
7. Ross AM, Gibbons RJ, Stone GW, Kloner RA, Alexander RW, for the AMISTAD-II ÂInvestigators. A randomized, double-blinded, placebo-controlled multicenter trial of adenosine as an adjunct to reperfusion in the treatment of acute myocardial infarction (AMISTAD-II). J Am Coll Cardiol 2005;45:1775–80.
8. Bullard AJ, Govewalla P, Yellon DM. Erythropoietin protects the myocardium against reperfusion injury in vitro and in vivo. Basic Res Cardiol 2005;100:397–403.
9. Hannon JP, Tigani B, Wolber C, et al. Evidence for an atypical receptor mediating the augmented bronchoconstrictor response to adenosine induced by allergen challenge in activity sensitized Brown Norway rats. Br J Pharmacol 2002;135:685–96.
10. Kin H, Zatta AJ, Lofye MT, et al. Postconditioning reduces infarct size via adenosine receptor activation by endogenous adenosine. Cardiovasc Res 2005;67:124–33.
11. Hinschen AK, RoseMeyer RB, Headrick JP. Adenosine receptor subtypes mediating coronary vasodilation in rat hearts. J Cardiovasc Pharmacol 2003;41:73–80.
12. Kaeffeer N, Richard V, Francois A, Lallemand F, Henry JP, Thuillez C. Preconditioning prevents chronic reperfusion-induced coronary endothelial dysfunction in rats. Am J Physiol 1996;271:H842–9.
13. M Shimizu, Miwa K, Hashimoto Y, Goto A. Encapsulating of chicken egg yolk immunoglobulin G (IgY) by liposomes. Biosci Biotechnol Biochem 1993;57:1445–9.
14. Kasuya T, Jung J, Kadoya H, et al. In vivo delivery of bionanocapsules displaying phaseolus vulgaris agglutinin-L(4) isolectin to malignant tumors overexpressing N-acetylglucosaminlyltransferase V. Hum Gene Ther 2008;19:887–95.
15. Kim YD, Fomsgaard JS, Heim KF, et al. Brief ischemia-reperfusion induces stunning of endothelium in canine coronary artery. Circulation 1992;85:1473–82.
16. Canyon SJ, Dobson GP. Protection against ventricular arrhythmias and cardiac death using adenosine and lidocaine during regional ischemia in the in vivo rat. Am J Physiol Heart Circ Physiol 2004;287:H1286–95.
17. Yaar R, Jones MR, Chen JF, Ravid K. Animal models for the study of adenosineÄreceptor function. J Cell Physiol 2005;202:9–20.
18. Norton ED, Jackson EK, Turner MB, Virmani R, Forman MB. The effects of intravenous infusions of selective adenosine A_1-receptor and A_2-receptor agonists on myocardial reperfusion injury. Am Heart J 1992;123:332–8.
19. Xu Z, Mueller RA, Park SS, Boysen PG, Cohen MV, Downey JM. Cardioprotection with adenosine A_2 receptor activation at reperfusion. J Cardiovasc Pharmacol 2005;46:794–802.
20. Vinten-Johansen J. Postconditioning: a mechanical maneuver that triggers biological and molecular cardioprotective responses to reperfusion. Heart Fail Rev 2007;12:235–344.
21. Lasic DD. Doxorubicin in sterically stabilized liposomes. Nature 1996;380:561–2.

Key Words: myocardial infarction ■ liposome ■ drug delivery system ■ adenosine.

2008K002A (2/2)

厚生労働科学研究費補助金
医療機器開発推進研究事業

循環器病治療機器の医工連携による研究開発・製品化・汎用化を実現するための基盤整備に関する研究（H20-医工-一般-002）

平成２０年度　総括・分担研究報告書

研究代表者　妙中　義之

平成２１（２００９）年４月

２／２冊

Annals of Biomedical Engineering, Vol. 37, No. 1, January 2009 (© 2008) pp. 82–93
DOI: 10.1007/s10439-008-9595-8

Computationally Managed Bradycardia Improved Cardiac Energetics While Restoring Normal Hemodynamics in Heart Failure

KAZUNORI UEMURA,[1] KENJI SUNAGAWA,[2] and MASARU SUGIMACHI[1]

[1]Department of Cardiovascular Dynamics, Advanced Medical Engineering Center, National Cardiovascular Center Research Institute, 5-7-1 Fujishirodai, Suita 565-8565, Japan; and [2]Department of Cardiovascular Medicine, Kyushu University Graduate School of Medical Sciences, Fukuoka 812-8582, Japan

(Received 9 September 2008; accepted 29 October 2008; published online 12 November 2008)

Abstract—In acute heart failure, systemic arterial pressure (AP), cardiac output (CO), and left atrial pressure (P_{LA}) have to be controlled within acceptable ranges. Under this condition, cardiac energetic efficiency should also be improved. Theoretically, if heart rate (HR) is reduced while AP, CO, and P_{LA} are maintained by preserving the functional slope of left ventricular (LV) Starling's curve (S_L) with precisely increased LV end-systolic elastance (E_{es}), it is possible to improve cardiac energetic efficiency and reduce LV oxygen consumption per minute (MVO_2). We investigated whether this hemodynamics can be accomplished in acute heart failure using an automated hemodynamic regulator that we developed previously. In seven anesthetized dogs with acute heart failure ($CO < 70$ mL min^{-1} kg^{-1}, $P_{LA} > 15$ mmHg), the regulator simultaneously controlled S_L with dobutamine, systemic vascular resistance with nitroprusside and stressed blood volume with dextran or furosemide, thereby controlling AP, CO, and P_{LA}. Normal hemodynamics were restored and maintained (CO; 88 ± 3 mL min^{-1} kg^{-1}, P_{LA}; 10.9 ± 0.4 mmHg), even when zatebradine significantly reduced HR (−27 ± 3%). Following HR reduction, E_{es} increased (+34 ± 14%), LV mechanical efficiency (stroke work/oxygen consumption) increased (+22 ± 6%), and MVO_2 decreased (−17 ± 4%) significantly. In conclusion, in a canine acute heart failure model, computationally managed bradycardia improved cardiac energetic efficiency while restoring normal hemodynamic conditions.

Keywords—Ventricular oxygen consumption, Mechanical efficiency, Specific bradycardic agent.

INTRODUCTION

Systemic arterial pressure (AP), cardiac output (CO), and left atrial pressure (P_{LA}) are three major variables necessary to guarantee survival. In the management of patients with acute heart failure following myocardial infarction or cardiac surgery, these variables have to be controlled within acceptable ranges.[1] Since the failing heart is in a critical state of myocardial energetics,[19] improvement of cardiac energetic efficiency is also essential in the management of such patients. Therapeutic interventions that enhance cardiac energetic efficiency have proven to be beneficial with respect to long-term outcome.[20] Reduction of heart rate (HR) has been shown to improve cardiac energetic efficiency.[6,26] However, in the failing heart, reduction of HR alone may decrease CO, and compromise hemodynamics.[5,13]

We previously demonstrated that AP, CO, and P_{LA} are determined by a mechanical equilibrium of the functional slope of Starling's curve (S_L) for the left ventricle (LV), systemic vascular resistance (R), and stressed blood volume (V).[30–32] Conversely, S_L, R, and V can be calculated from AP, CO, and P_{LA}, indicating that a set of AP, CO, and P_{LA} values uniquely corresponds to a set of S_L, R, and V values. When HR is reduced, the three variables of AP, CO, and P_{LA} can only be maintained by increasing LV contractility (LV end-systolic elastance, E_{es}) to offset HR reduction and to preserve S_L (see *Theoretical analysis* in "Materials and Methods"). In this hemodynamics, total mechanical energy of LV contraction, which is indicated by LV pressure–volume area (PVA), also increases with HR reduction. Increases in both E_{es} and PVA elevate LV oxygen consumption per beat (BVO_2).[28,29] However, since the increase in the external work done by LV is greater than the increase in BVO_2, cardiac energetic efficiency is improved. Furthermore, LV oxygen consumption per minute (MVO_2) decreases because the reduction in HR is sufficient to compensate for the increase in BVO_2.

To realize the above hemodynamics (optimal hemodynamics) in patients with acute heart failure, AP, CO, and P_{LA} should be controlled under HR

Address correspondence to Kazunori Uemura, Department of Cardiovascular Dynamics, Advanced Medical Engineering Center, National Cardiovascular Center Research Institute, 5-7-1 Fujishirodai, Suita 565-8565, Japan. Electronic mail: kuemura@ri.ncvc.go.jp

reduction by regulating infusions of multiple cardiovascular drugs such as inotropes and vasodilators. However, the control process is difficult and time-consuming, since the responses of AP, CO, and P_{LA} to these drugs vary between patients and within patient over time, and the responses are interrelated.[9,23] We previously demonstrated that it is possible to control AP, CO, and P_{LA} stably and accurately by directly controlling S_L, R, and V with cardiovascular drugs, due to their mechanical equilibrium.[30] This strategy is feasible because the responses of S_L to inotropes, R to vasodilators, and V to volume expander or diuretics are relatively invariable.[30] Furthermore, these three input–output relations; namely, inotrope–S_L, vasodilator–R, and volume expanders/diuretics–V are effectively decoupled. We hypothesized that this approach would be especially efficacious in accomplishing optimal hemodynamics in acute heart failure. Under HR reduction, an excessive increase in E_{es} will compromise the cardiac energetic efficiency.[15] Therefore E_{es} should be increased to a precise level. This can be done through a tight control of the inotrope–S_L relation. Although inotropes also affect R or V,[3,7] these effects can easily be compensated by the vasodilator–R and volume expanders/diuretics–V relations.

The purpose of this study was to prove the hypothesis that direct control of S_L, R, and V under HR reduction attains the optimal hemodynamics and at the same time improves cardiac energetic efficiency and reduces MVO_2 in a canine model of acute heart failure, as predicted in *Theoretical Analysis*. An automated hemodynamic regulator that we developed previously[30] was used to directly control S_L, R, and V. The regulator directly controls S_L with dobutamine (DOB), R with sodium nitroprusside (SNP), and V with dextran (DEX) and furosemide (FUR), thereby controlling AP, CO, and P_{LA}. To reduce HR, we used a specific bradycardic agent, zatebradine (UL-FS49) that specifically reduces HR without affecting LV contractility.[12,24]

MATERIALS AND METHODS

Theoretical analysis

S_L is theoretically determined by E_{es}, HR, R, and diastolic myocardial stiffness (k), and can be expressed by the following formula[31]:

$$S_L = \frac{1}{k} \cdot \frac{E_{es}}{(E_{es}/HR) + R} \tag{1}$$

Equation (1) can be rewritten as follows:

$$E_{es} = \frac{S_L \cdot k \cdot R}{1 - S_L \cdot k/HR} \tag{2}$$

The external work done by LV is represented by stroke work (SW) and expressed as[11]

$$SW = (P_{es} - P_{ed}) \cdot CO/HR \tag{3}$$

where P_{es} is LV end-systolic pressure and P_{ed} is end-diastolic pressure. In the LV pressure–volume diagram, PVA is the area circumscribed by the end-systolic pressure volume relation, the end-diastolic pressure volume relation, and the systolic pressure volume trajectory of LV. PVA, an index of total mechanical energy of LV contraction, is the sum of potential energy and external work of LV,[28,29] and can be expressed as

$$PVA = P_{es} \cdot P_{es}/2E_{es} + SW \tag{4}$$

If we approximate P_{es} to AP and P_{ed} to P_{LA}, SW and PVA can be expressed as

$$SW = (AP - P_{LA}) \cdot CO/HR \tag{5}$$

$$PVA = AP \cdot AP/2E_{es} + SW \tag{6}$$

BVO_2 is related to PVA and E_{es} as follows[28,29]:

$$BVO_2 = \alpha \cdot PVA + \beta \cdot E_{es} + \gamma \tag{7}$$

where α, β, and γ are constants representing oxygen cost of PVA, oxygen cost of contractility, and basal metabolism, respectively. MVO_2 is expressed as follows:

$$MVO_2 = BVO_2 \cdot HR \tag{8}$$

Using Eqs. (2–8) and fixed values of AP, CO, and P_{LA} (Table 1), we numerically simulated the individual relations of HR with E_{es}, SW, PVA, BVO_2, LV mechanical efficiency (ME) and MVO_2 (Fig. 1). In these computations, representative k, α, β, and γ values (Table 1) were used, which are appropriate for a 20-kg dog.[10,29] In Eq. (2), S_L was calculated from the ratio of CO to logarithmic function of P_{LA} as described

TABLE 1. Values of the parameters used in *Theoretical Analysis*.

Parameters	Values
AP, mmHg	100
CO, mL min^{-1} kg^{-1}	100
P_{LA}, mmHg	10
k, mL^{-1}	0.082
α, mL O_2 · mmHg^{-1} · mL^{-1}	1.8×10^{-5}
β, mL O_2 · beat^{-1} · mmHg^{-1} · mL	0.0018
γ, mL O_2 · beat^{-1}	0.01

AP, systemic arterial pressure; CO, cardiac output; P_{LA}, left atrial pressure; k, left ventricular diastolic myocardial stiffness; α, oxygen cost of pressure–volume area; β, oxygen cost of contractility; γ, constant representing basal metabolism.